MULTI-FRAGMENTATION AND DISAPPEARANCE OF FLOW IN INTERMEDIATE ENERGY HEAVY-ION COLLISIONS

By

TONG QING LI

A DISSERTATION

Submitted to
Michigan State University
in partial fulfillment of the requirements
for the Degree of

DOCTOR OF PHILOSOPHY

Department of Physics and Astronomy

1993

ABSTRACT

MULTI-FRAGMENTATION AND DISAPPEARANCE OF FLOW IN INTERMEDIATE ENERGY HEAVY-ION

By

Tong Qing Li

The equation of state (EOS) of nuclear matter can be probed through heavy ion reactions if finite size effects are taken into account. A first-order liquid-gas phase transition and the critical point, if measured, can provide a calibration point for EOS.

The critical behavior of nuclear fragmentation is characterized by a power law cluster mass distribution. The measured Z-distributions of fragments emitted from central collisions of ^{40}Ar + ^{45}Sc at beam energies from 15 to 115 MeV/nucleon have been fitted to power laws $\sigma(Z) \propto Z^{-\lambda}$. The apparent exponent, λ, reaches a minimum at a beam energy of 23.9 ± 0.7 MeV/nucleon. A percolation model calculation reproduces the observed Z-distributions for all beam energies, using the mean excitation energy as extracted from proton kinetic energy spectra. We extract the critical value of the deposited excitation energy for our system and make predictions for the dependence of this quantity on the size of the fragmenting system. The asymptotic limit of the critical temperature for a binding energy of 8 MeV/nucleon is found to be 13.1 ± 0.6 MeV using percolation calculations. The asymptotic critical point can be used as a constraint for the EOS of nuclear matter.

Dynamically the EOS can be probed by collective motion. At low beam energies ($\sim$ 10MeV/nucleon), the dominant interaction in the reaction zone is the attractive

MULTI-FRAGMENTATION AND DISAPPEARANCE OF FLOW IN INTERMEDIATE ENERGY HEAVY-ION COLLISIONS

By

TONG QING LI

A DISSERTATION

Submitted to
Michigan State University
in partial fulfillment of the requirements
for the Degree of

DOCTOR OF PHILOSOPHY

Department of Physics and Astronomy

1993

ABSTRACT

MULTI-FRAGMENTATION AND DISAPPEARANCE OF FLOW IN INTERMEDIATE ENERGY HEAVY-ION

By

Tong Qing Li

The equation of state (EOS) of nuclear matter can be probed through heavy ion reactions if finite size effects are taken into account. A first-order liquid-gas phase transition and the critical point, if measured, can provide a calibration point for EOS.

The critical behavior of nuclear fragmentation is characterized by a power law cluster mass distribution. The measured Z-distributions of fragments emitted from central collisions of $^{40}Ar + ^{45}Sc$ at beam energies from 15 to 115 MeV/nucleon have been fitted to power laws $\sigma(Z) \propto Z^{-\lambda}$. The apparent exponent, λ, reaches a minimum at a beam energy of 23.9 ± 0.7 MeV/nucleon. A percolation model calculation reproduces the observed Z-distributions for all beam energies, using the mean excitation energy as extracted from proton kinetic energy spectra. We extract the critical value of the deposited excitation energy for our system and make predictions for the dependence of this quantity on the size of the fragmenting system. The asymptotic limit of the critical temperature for a binding energy of 8 MeV/nucleon is found to be 13.1 ± 0.6 MeV using percolation calculations. The asymptotic critical point can be used as a constraint for the EOS of nuclear matter.

Dynamically the EOS can be probed by collective motion. At low beam energies ($\sim$ 10MeV/nucleon), the dominant interaction in the reaction zone is the attractive

mean field, which leads to a negative dynamical deflection (flow) of the final particles. At high beam energies ($\sim$ 400MeV/nucleon), the dominant interaction is the nucleon-nucleon (n-n) repulsive interaction, which leads to a positive deflection (flow) of the final products. The balance energy is the beam energy at which the mean field attraction is balanced by the n-n repulsion. This balance energy compared with dynamical calculation such as the Boltzmann-Uehling-Uhlenbeck (BUU) model can provide constraints on the EOS.

We observed the balance energy of Ar + Sc to be 87 ± 12 MeV/nucleon. A single observation of central collisions of one system apparently cannot give strong constraints on EOS.

Dedicated with love to Michelle and Dillon.

ACKNOWLEDGEMENTS

I wish to thank my thesis advisor, Gary Westfall, for his encouragement and patience during all the ups and downs over the years. It is his advise, guidance and teaching that made the four years of research challenging and full of fun; and it is his sense of humor that made the work fabulously enjoyable (not all the time of course) and rewarding.

A special thanks to Wolfgang Bauer for his support of my change from doing theory to doing experiments and for his constant support and advice in the theoretical aspects of the research.

I also owe a deep debt to all of my 4π colleagues: Roy Lacey's "plans" and discussions, our hot debate and our downstairs rush for scheduled runs, leaves an unerasable memory; Skip Vander Molen, his "call me now" spirit on running experiment; Ken Wilson's enthusiastic and patient discussions, his leading role on research made my first year a lot easier and fun; Sherry Yennello, her advise over all aspects of my graduate student "life" (if we have any), from physics to every day problems, are invaluable; Jaeyong Yee, for his silent support and over night hard work; Gene Gualtieri, for his jokes and his patience of listening to all of my problems; Darren Craig, for his working on everything for four dollars an hour spirit and his contribution to all aspects of this thesis work are highly acknowledged;

Special thanks to all the lab directors, Sam Austin, Konrad Gelbke and Walt Benenson, for their financial support on the research, travel to conferences and summer schools, and for their excellent management, which makes the lab a most productive one.

I also wish to express my appreciation to all of my colleagues at the NSCL: John Yurkon and Dennis Swan, on their supervision in making detectors; most of all, their

friendly help made the working downstairs a lot of fun. Len Morris and Steve Bricker, for their support on mechanical work of the detectors and their cooperative spirit; Jim Vincent, our electronic life saver; Cyclotron operating staff for their patience to hear "where is the beam" millions of times; all the secretaries and staff, they make the NSCL an easy, comfortable and fun place to work.

Most of all, I owe great debt to my parents. It is their encouragement, their endless support and their love that made me who I am and made my pursuit in physics possible; to my wife, whose love, patience and understanding made the final finishing of my thesis a lot of easier; and my son, Dillon, whose midnight crying made this thesis a little late but a much more colorful part of my life.

Contents

List of Tables

List of Figures

Chapter 1

Introduction

The first heavy ion accelerator that made heavy ion reaction studies possible at beam energy of 1 GeV per nucleon was the Princeton-Penn Accelerator in 1972 [Gupt93]. When the Bevatron, a weak focusing synchrotron which could produce 6.2 GeV protons, was coupled with the SuperHILAC, a linear accelerator which could accelerate heavy ions to 8 MeV/nucleon, the Bevalac at Berkeley went into operation. Heavy ions could be accelerated at the Bevalac up to 2.1 GeV/nucleon [Gupt93, Gutb89a]. The high energy nucleus bombarding the target nucleus can create high excitation and high pressure. Nuclear matter with densities as high as 2 to 4 times the nuclear saturation density can be studied in a controlled laboratory environment. These studies may provide reliable information towards the bulk properties of nuclear matter at high density as studied by astronomical observations in neutron stars and supernovas. Heavy ion reactions turned the attention of nuclear physicists from the structure of nuclei to the bulk properties of nuclear matter. The first goal is simple and clear – the determination of the equation of state (EOS) of nuclear matter.

The difficulties of measuring the EOS of nuclear matter are due to the fast time scale and small space scale, which make direct time-dependent measurements impossible. Only final products are measured with a given detector acceptance. The microscopic process of heavy ion reactions can not be observed directly. Thus, the

picture of the time evolution of a reaction system largely relies on theories. Heavy ion reactions increase the number of participating particles to the order of 10^2 comparing with proton-proton collision, but the particle number scale is far from the macroscopic situation of 10^{23} particles. The macroscopic observables such as temperature, pressure, entropy, etc. either have large fluctuation in the finite size system or have different physical meanings. The finite size, which cause large fluctuations in all the statistical quantities, makes the study of the EOS difficult.

1.1 Nuclear Matter Compressibility

Due to the high energy and short time scale, it is difficult to measure directly macroscopic quantities such as volume, and pressure. Therefore, it is impossible to directly measure the thermodynamic properties of nuclear matter as we could in the classical case. Astronomical observations indicate that such highly compressed, highly excited systems do exist in supernova and neutron stars.

The properties of the nuclear EOS are discussed in terms of nuclear compressibility, which represents the hardness of nuclear matter against compression. Hence, the nuclear compressibility is measured, or estimated, from secondary observables compared with theoretical models. Putting all possible constraint on the nuclear compressibility is essential to both nuclear physics and astrophysics. The Landau theory of Fermi liquids gives a K from 74 to 371 MeV [Brow85]. The study of giant monopole resonance, which corresponding a compressional mode of the nucleus, showed that $K \sim 210 \pm 30$ MeV [Blai80]. The droplet model of nuclear masses suggests K from 210 to 410 MeV. The dynamic study of Bevalac energy collective flow showed a compressibility of 380 MeV [Krus85] using BUU model which incorperates nucleon-nucleon collisions and a mean field with no momentum dependent

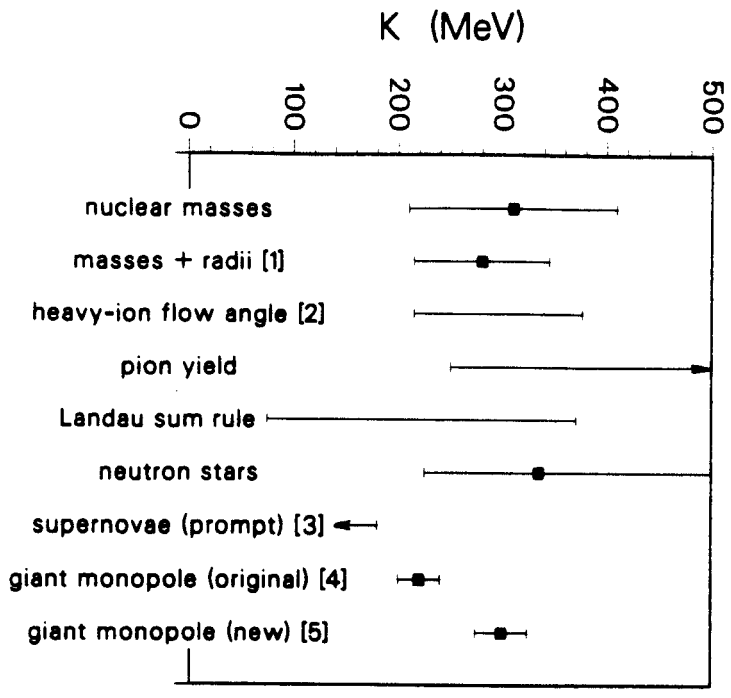

Figure 1.1: Nuclear compressibility obtained from different studies. (from reference [Glen88]). Reference [1] to [5] are listed in [Glen88].

terms. Later study using BUU calculation with momentum dependent mean field indicated a compressibility of 215 MeV [Gale90]. Glendenning summarized all the different studies of the nuclear compressibility and plotted the result shown in Figure 1.1 [Glen86].

Intermediate energy heavy ion physics exhibits many transitional phenomena which may provide more information concerning nuclear compressibility. At this energy, the excitation is high enough to break apart the nucleus but is not high enough to totally disintegrate it into its component nucleons. A transition from sequential decay where the hot nuclear system decays through a binary decay chain to multifragmentation where the system breaks up in a fast time scale may occur. Or a transition from fission-evaporation process, which indicates a liquid-gas coexistence,

to a critical point at which the system evaporates totally with no heavy residue may be possible. A first order liquid-gas phase transition terminates at a critical point.

Different from statistical systems, there is also a strong dynamical process involved in heavy ion reactions. The entrance projectile incedent on the target nucleus with a certain impact parameter and velocity is a unique initial condition which leads the evolution of the reaction system both statistically and dynamically. Some strong collective motion such as transverse flow, azimuthal distributions and rotation have been observed [Gutb89a, Gutb89b, Wils91, Lace93]. The dynamic collective flow changes direction in this energy region, which indicate a competition between nucleon-nucleon repulsive and meanfield attractive interactions. The dynamical observations provide information on the interactions between particles in the reaction zone. Therefore, the search for the EOS of nuclear matter is in two inseparable directions: statistical studies and dynamical studies.

1.2 Statistical Behavior of Heavy Ion Reaction

High energy heavy ion reactions are successfully described by the statistical fireball model which assumes the projectile nucleus interacting with the target creates a fireball and target and projectile spectators. [West76, Goss77, West82, Jaca87] (see Figure 4.5). Due to the high excitation energy, the reaction system can be disintegrated into light particles. At low beam energies (below 8 MeV/nucleon), the reaction process is dominated by fusion-fission and light particle evaporation. It is in the intermediate energy region, the beam energy from 10 to several hundred MeV per nucleon, that there is a transition from binary fission-evaporation and sequential decay processes to multi-fragmentation processes. Multi-fragmentation is defined as the simultaneous emission of heavy particles ($Z \geq 3$). Theoretical studies based on statistical de-

scriptions indicate that in the intermediate energy region the heated and compressed reaction system goes through the mechanical instability region during the expansion where the system disintegrates simultaneously [Good84, Boal86]. On the pressure vs. density plot, during the expansion, the system goes through the liquid-gas co-existence region (see Figure 4.2) since the nuclear equation of state resembles the properties of classical Van der Waals gas. There is a second order phase transition characterized by a critical point. Below the critical point, the liquid-like compound system may evaporate light particles or fission while above the critical point, the system may totally break up into light particles [Good84, Jaqa84, Boal86, Pana84, Kapu84, Bond85].

There are two extreme approaches in statistical theories, the sequential decay approach and the simultaneous breakup approach [Frie89, Lópe89, Cebr90a] in describing the heavy ion reactions. In the sequential statistical theory, one assumes that the compound system de-excites through a sequence of binary breakups. The final fragments are the sum of the chain binary decay. The decay rates are assumed to be given by detailed balance [Frie89]. While simultaneous emission assumes a statistical ensemble (canonical or micro canonical), the fragments are in equilibrium with each other as the system expands. The two approaches are illustrated by Figure 1.2.

It is observed that at low beam energies (below 10 MeV/nucleon), the particle emission is dominated by binary sequential decay, while at high energies, the multifragmentation takes place [Cebr90a, Cebr90b, Biza93] Determination of onset of multifragmentation has been a major research effort in the last five years [Boug88, Yenn90, Bowm91, Blum91, Yenn91, Ogil91, Hube91, Bowm92, Kim92, Sang92, Hage92, Grab92, Ogil93, Peas92]. To discriminate the two different statistical processes, observables which are sensitive to the evolution of the system are necessary. The study of the phase space event shape of the emission particles, parameterized by sphericity and coplanarity [Cebr90a], can distinguish the transition from sequential decay to si-

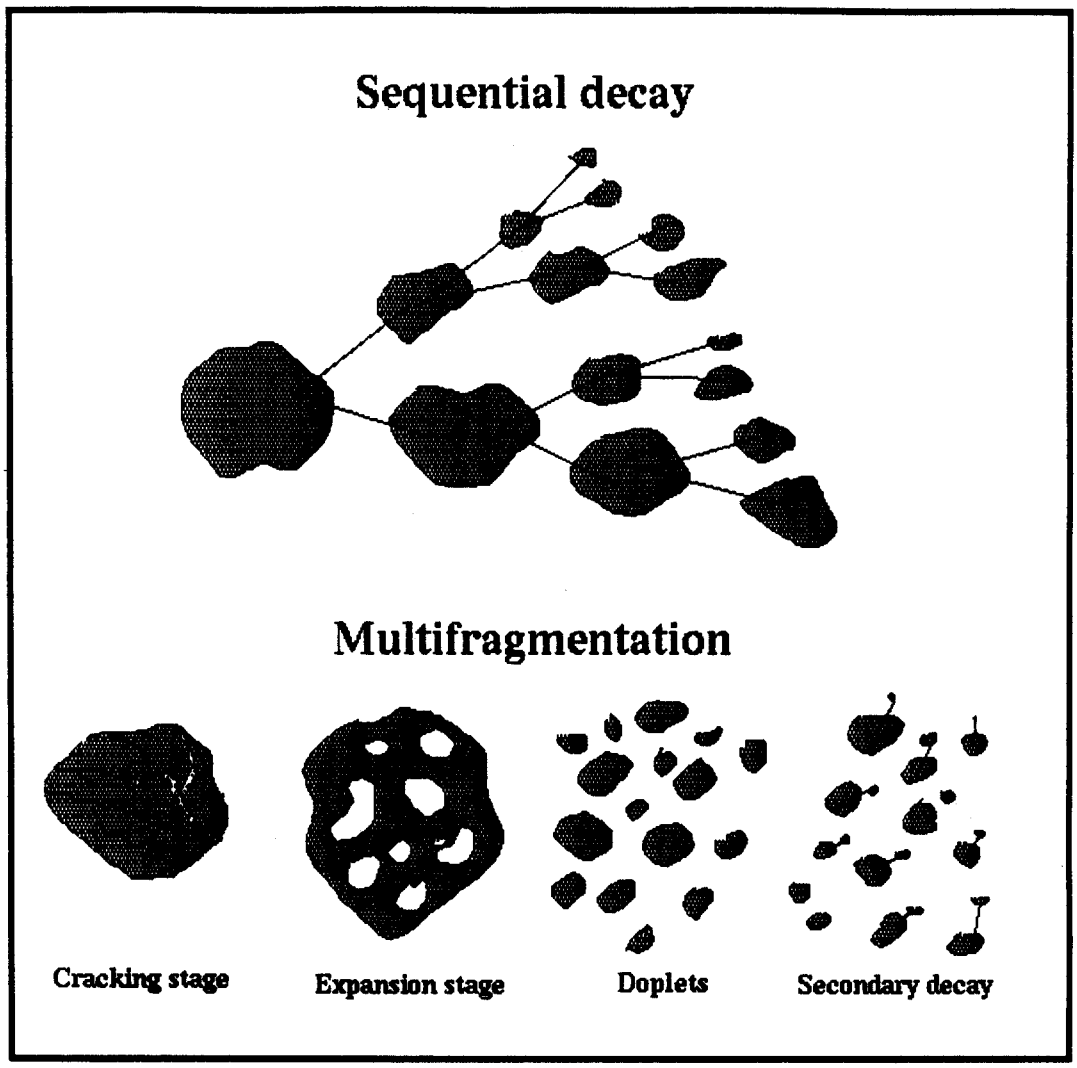

Figure 1.2: Two statistical approaches for nuclear fragmentation

multaneous emission. Because binary sequential decay has an elongated pattern in momentum space, while simultaneous emission is more isotropic [Cebr90a], the onset of multifragmentation can be observed by studying the event shapes for a variety of beam energies [Cebr90a].

Also associated with the statistical properties of heavy ion reaction is the liquid-gas phase transition of nuclear matter, which has been predicted in the intermediate energy region for decades [Küpp74, Saue76, Lamb78, Jaqa84, Good84, Pana84, Kapu84, Bond85, Boal86]. The similarity of nucleon-nucleon interaction with the interaction of Van der Waals gas suggests a critical behavior of bulk nuclear matter may exist [Abra79]. The nuclear EOS derived from two body interactions using a variety of methods all show the first order liquid-gas phase transition terminating at a critical point. Recently, the results of inclusive fragment production of high energy proton induced reactions stimulated wide spread interests [Finn82, Mini82, Hirs84, Hüfn85].

The observable for studying the liquid-gas phase transition is the mass distribution of the final reaction products. Both Fisher's droplet model [Fish67, Pana84, Pori89] and percolation theory [Stau79, Baue85, Baue88] predict that the cluster distribution has a power law form in the vicinity of the critical point. At the critical point, the exponent of the power law goes to a minimum. The measured critical point can be used to constrain the EOS if finite size effects are considered.

From the EOS of nuclear matter, the critical point can be obtained by setting the first and second derivative of pressure to nucleon density equal to zero (see section 4.1.1). Therefore, determination of the critical point using the cluster distributions can provide information about the EOS of nuclear matter. Both inclusive measurements of proton and light ion induced reactions showed the power law behavior and the proton induced reaction showed a minimum of the power law exponent [Pori89, Hirs84, Finn82, Chit83, Yenn90].

However, the inclusive measurements are integrated over impact parameters leading to different types reactions with different excitation energies. To obtain unambiguous evidence of such critical phenomena for a finite system, more exclusive measurements must be done and, most importantly, the finite size effects have to be treated [Jaqa84].

To obtain unambiguous measurements of the statistical properties, especially the transitional properties such as sequential decay to multifragmentation, or the liquid-gas phase transition, better exclusive measurements are necessary. Because the initial conditions such as impact parameter and reaction plane, and excitation energy can be estimated using exclusive measurements, the study of central collisions will provide unambiguous statistical information.

1.3 Dynamical Behavior

Dynamical collective motion has been observed in heavy ion reactions [Gutb89b]. The averaged phase space distributions show some non isotropic properties, such as transverse momentum flow, squeeze out and rotation [Gutb89a, Krof89, Krof91, Wils90, Wils91, Krof92]. Dynamical collective motion may provide information concerning the interactions inside the reaction zone. Dynamical model calculations show the gross features of the collective motion of heavy ion reactions. The most successful dynamical model, the Boltzmann-Uehling-Uhlenbeck (BUU) transport equation calculation [Bert88, Gale90, Pan93], which incorporates the mean field of nuclear matter and nucleon-nucleon collisions, reproducs the observed transverse momentum flow [Ogil90, Gale90, Krof92, Pan93].

At intermediate energies, the nucleon-nucleon hard core repulsion competes with the mean field attraction. At low beam energy, the mean field attraction is stronger

than nucleon-nucleon repulsion and a negative deflection of the final reaction products will occur. At high beam energy, the nucleon-nucleon repulsive collision dominates the reaction, and a positive deflection of the final reaction products will be observed. At a certain beam energy (depending on the mass of the reaction system), if the mean field attraction is balanced by nucleon-nucleon repulsion, the flow will disappear. The energy at which the transverse flow disappears is called the balance energy, which can be used to determine the mean field parameters. In BUU, the EOS is linked with the mean field [Bert88]. Comparing the experimentally measured balance energy with the theoretical calculation, we can gain information about the mean field and therefore the EOS.

The balance energy calculated by BUU is strongly sensitive to the medium nucleon-nucleon cross sections which is a parameter of the nucleon-nucleon collisions of the BUU calculation, but it is weakly sensitive to the nuclear compressibility. The single measurement of balance energy does not provide a complete constraint on the input used by BUU. In order to obtain complete constraint on the input parameters of BUU, we must do measurements of the balance energy for different reaction systems and measurements of the impact parameter dependence of the balance energy [West93, Sull90].

1.4 Organization of the Thesis

The main objective of this thesis is to probe the nuclear EOS by studying the properties of the statistical breakup of the reaction system and dynamical collective motion.

The thesis concentrates on the experiment of ^{40}Ar + ^{45}Sc at 15, 25, 35, 45, 65, 75, 85, 95, 105 and 115 MeV/nucleon. The main goal of the experiment is to study the onset of multifragmentation and the liquid-gas phase transition [West88]. The

MSU 4π Array can exclusively characterize the collisions. Only central collisions are studied in this thesis. In chapter 2, the experimental set-up, particle identification and data reduction are discussed in detail.

Before the statistical and dynamical results can be addressed, the initial condition of the reaction, i.e. impact parameter and reaction plane, must be determined. In chapter 3, the event characterization is discussed. The impact parameter is determined by an analytical formula which links the impact parameter to global observables using the probability density distribution of the global observable. To obtain a common centrality cut for all studies with minimum bias, a combined global observable is proposed. Then the method of reaction plane determination, the azimuthal correlation method, is introduced. A comparison with the previously used transverse momentum method shows that a better measurement of reaction plane is given by the azimuthal correlation method.

Multifragmentation is discussed in chapter 4. Observed Z-distributions are corrected for the detector acceptance. These distributions are related to critical behavior. Then a percolation calculation, linking the bond breaking probability to the proton kinetic energy slope parameter is presented. Comparing with the GSI experiment of Au + C, Al, Cu at 600 MeV per nucleon [Ogil91], the percolation calculation shows the mass dependence of critical behavior. To estimate the finite size effects, we run the percolation calculation increasing the size of the initial system. The asymptotic limit of the critical point that has been obtained for a binding energy of 8 MeV per nucleon is $T_c = 13.1 \pm 0.6$ MeV.

In chapter 5, we discuss the dynamics of the nearly symmetric system in terms of transverse flow and the disappearance of the flow. Comparing with the BUU calculation, the nuclear compressibility be discussed.

Chapter 6 will summarize the results.

Chapter 2

Experiment

2.1 Introduction

The experiment was done at the National Superconducting Cyclotron Laboratory (NSCL) of Michigan State University (MSU) with MSU 4π Array. The newly finished Bragg Curve Counters (BCC) working in ion chamber mode (as ΔE with the fast plastic phoswich working as E) gave a lower energy threshold and good charge resolution for $2 \leq Z \leq 13$. The BCCs combined with the fast/slow phoswichs provided a wide range of Z (charge number from 1 to 13) identification and large dynamic range (3 MeV/nucleon to ~200 MeV/nucleon for Helium) and nearly 4π sr solid angle coverage [West85, Li93]. To study nuclear matter in a highly compressed and excited environment, a nearly symmetric beam and target combination was chosen to eliminate the projectile and target spectator components in head on (central) collisions. A wide range of beam energies (15 to 115 MeV/n) was used to cover the range of temperatures of nuclear matter at which a liquid-gas phase transition predicted by theories may occur.

The following is a summary of the experiment:

Goal: Multi-fragmentation: Liquid-Gas phase transition.

Disappearance of flow: Balance energy.

Experiment No: NSCL EXPT. 88016

Reaction: $^{40}Ar + ^{45}Sc$

Beam: ^{40}Ar of 15, 25, 35, 45, 65, 75, 85, 95, 105, 115 MeV/nucleon
of about $0.1pnA$ produced by NSCL K1200 cyclotron
at charge state from 10^+ to 16^+.
The K1200 cyclotron operation parameters are shown in table 2.1.

Target: Mounted on the rotary target frame
1.6 mg/cm^2 ^{45}Sc self supporting target

Detectors: MSU 4π Array (Phase II):
- 170 Ball Phoswich Telescopes (BALL)
- 45 Forward Array Telescopes (FA)
- 55 Bragg Curve Counters (BCC)

Triggers: S_2 - system 2 trigger: any two ΔE of Ball and FA firing.
S_5 - system 5 trigger: any five ΔE of Ball and FA firing.

Table 2.1 is a summary of the beams produced by K1200 cyclotron. The charge state of Ar ions generated by the electron cyclotron resonance (ECR) source was from 10^+ for 45 MeV/nucleon to 16^+ for 115 MeV/nucleon. The cyclotron was operated at a radio frequency (RF) from 14.2 MHz to 21.5 MHz corresponding to a period of 46.5 ns to 70.4 ns for the beam burst.

2.2 Michigan State University 4π Array

Enclosed in an aluminum 32 face truncated icosahedron (soccer ball geometry with 12 pentagonal faces and 20 hexagonal faces) with a diameter (from hexagon to hexagon outer surface) of 241.3 cm, the detectors are mounted on the 2 cm thick aluminum

Table 2.1: Ar beam produced by K1200 cyclotron.

E_{beam}	charge state	f
(MeV/n)		(MH_z)
115	16^+	21.5
105	16^+	20.8
95	14^+	19.9
85	14^+	19.0
75	18^+	19.0
65	12^+	16.8
45	10^+	14.2
35	18^+	14.2

back plates – 10 pentagons and 20 hexagons, leaving two pentagons as beam entrance and exit. Each of the 30 back plates supports a detector module composed of close packed triangular pyramid shaped fast/slow plastic phoswich detectors (5 detectors for a pentagonal module and 6 for a hexagonal module) [West85, Cebr90a, Wils91]. A BCC is mounted in front of the phoswich detectors of each module. A schematic drawing of a pentagonal module is shown in Figure 2.1. In the forward direction, 45 fast/slow plastic phoswich telescopes were mounted in the exit pentagonal area covering the angular range of 7° to 18° with a solid angle coverage of 51%. This set of detectors is referred to as the forward array (FA).

Table 2.2 shows the main specifications of the three types of detectors. In column 1, the angle range is the polar angle the detector array covers with respect to beam direction. The solid angle coverage means the percentage of the solid angle the detector array covers with respect to full solid angle within the angular range specified. The energy threshold is the lowest kinetic energy the detectors can detect for different particles. We only show proton, helium and carbon as examples. The phoswich telescopes (both BALL and FA) can separate Z=1 isotopes, proton, deuteron and triton. The gain of BALL phoswich detectors was set to accept Z=1 to Z=8 and FA

Table 2.2: MSU 4π Array Detector Parameters.

Specification	Ball Phoswich	FA Phoswich	BCC
Angle Range (degree)	23 to 157	7 to 17	23 to 157
Solid Angle Coverage(%)	83	47	83
Z identification	Z=1 to 8 †	Z=1 to 13 †	Z=2 to 12 ‡
Energy Threshold(MeV/n):			
Proton	11	12	-
Helium	15	12	3
Carbon	27	21	4

† Both BALL and FA phoswich has Z=1 isotope resolution. (p, d, t).

‡ The BCC gain is set to accept $2 \leq Z \leq 12$

phoswich to accept Z=1 to Z=13 and BCC can identify Z=2 to Z=12.

2.3 Bragg Curve Counter

The bragg curve spectrometer was first proposed by Gruhn et al [Gruh82], then studied and improved by others [Schi82, Asse82, Oed83a, Oed83b, Mcdo84, Moro84, Shen85, Kott87, Cebr91]. The BCC has several advantages: It has a low energy threshold; It can be made to subtend large solid angle with good Z resolution and linear energy response. The particles go through an electric field parallel to the path of the particle which is especially suitable for a spherical geometry where particles emitted from the target go through an radial field inside the BCC. To accomplish the goal of maximizing the solid angle coverage and minimizing the low energy cut off, hexagonal or pentagonal pyramid G10 fiberglass casings are mounted directly on the phoswich module to make a close-packed detector array inside the 4π Array. A 2.5 μm thick aluminum coating is evaporated on the entrance surface of the phoswich module which serves as the BCC anode. The anodes on the first ring of five hexagonal modules (the first ring from the beam axis) are further segmented into six segments

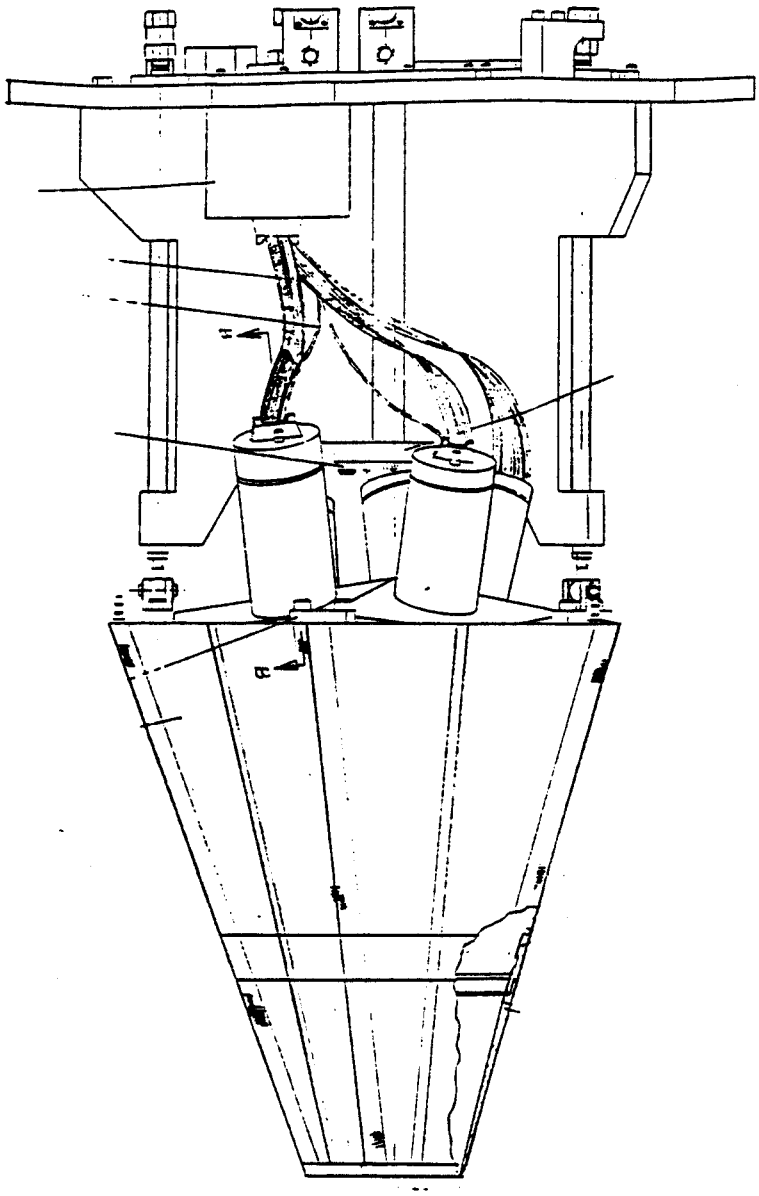

Figure 2.1: A pentagon module of MSU 4π array.

which give six independent outputs corresponding to the six phoswich telescopes. The entrance window is made up of a 900 $\mu g/cm^2$ thick, aluminized kapton which was epoxy-bonded on a stainless steel window frame with 1 cm spacing supporting grid. The distance between the cathode and the anode is 13.36 cm .

A Frisch grid made of 12.5 μm gold plated tungsten wires with a 0.5 mm spacing is epoxy-bonded with silver epoxy on a G10 frame with a conducting copper strip. The Frisch grid to anode distance is 1 cm. The Frisch grid is connected to ground potential to shield the positive ion induced charge. On the inside surface of the G10 BCC cover, 21 field shaping copper strips are installed. The 21 strips are linked by twenty-one 1.55 MΩ resistors from Frisch grid to the cathode to provide a radial electric field. A layer of silver conducting paint covers the BCC and is connected to ground to shield the detector from the electromagnetic interference. The BCCs are filled with P5 gas (95% Ar and 5% CH_4) with a pressure of 500 torr. The anode potential is set at +200 V and cathode at -1200V. The distance from the entrance window of BCC to the target is 17.27 cm. The entering charged particles ionize the gas and produce electron-ion pairs. The electrons and ions drift along the radial field in opposite directions. Taken from anode, the BCC signal feeds into a charge-sensitive pre-amplifier mounted on each module inside the vacuum chamber to reduce the signal to noise ratio. An integrated signal is obtained at the output of the pre-amplifier. The schematic of the preamplifier is shown in figure 2.3. The signal is further amplified by a shaping amplifier. The shaping amplifier gives a differentiated fast signal whose peak is proportional to the charge and an one stage differentiation and two stages of integration of the slow signal whose peak is proportional to the energy deposited by the detected particle. The time constant of the slow signal is $5\mu s$. The slow signals go into peak sensing ADCs (Silena 4418/v). The NSCL data acquisition system is used to read the ADCs.

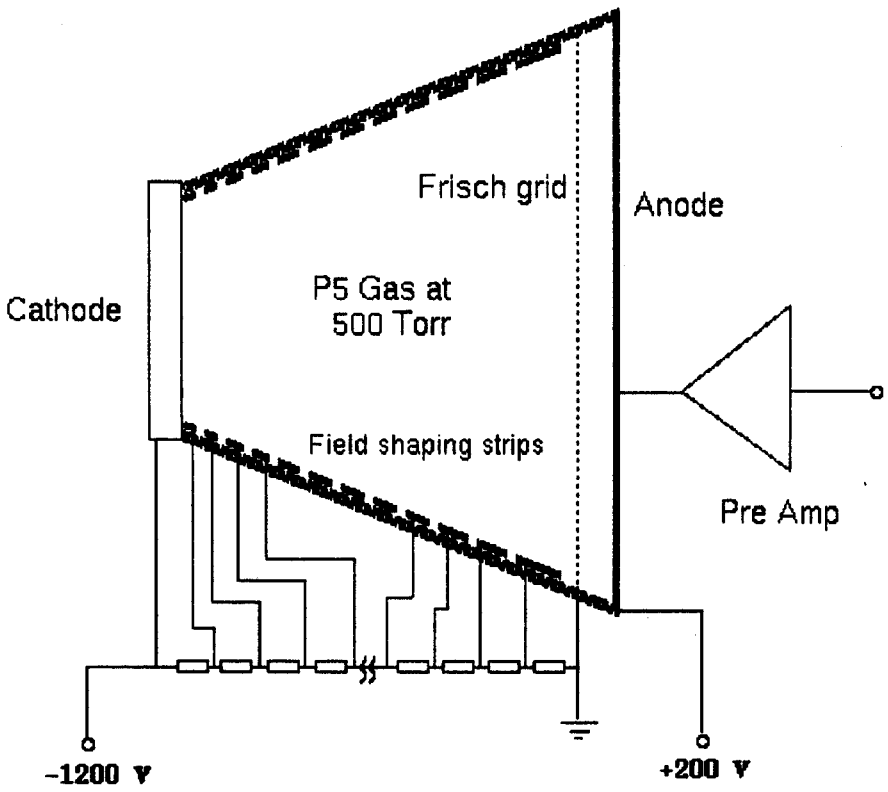

Figure 2.2: Schematic diagram of the MSU 4π Bragg Curve Counter (BCC).

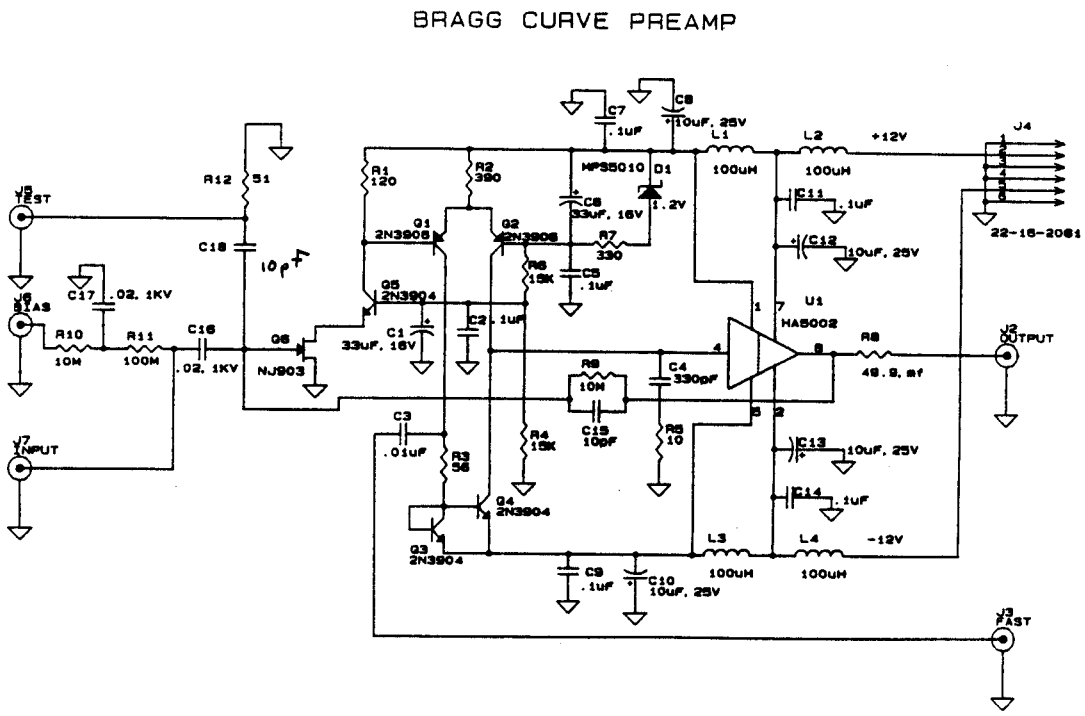

Figure 2.3: Schematic of the preamplifier used for the Bragg Curve Counters.

2.4 Phoswich detectors

The 170 ball fast/slow plastic telescopes are made of 3 mm thick Bicron BC-412 fast plastic scintillator with a rise time of 1.0 ns and a fall time of 3.3 ns optically coupled to a 25 cm thick BC-444 slow plastic scintillator with a rise time of 19.5 ns and a fall time of 179.7 ns. The ball hexagonal modules each cover a solid angle of 6×65.96 msr and the pentagon module covers a solid angle of 5×49.92 msr. The 45 forward array telescopes are made of the same fast/slow plastic as the ball phoswich detectors except that the fast plastic ΔE counters are 1.6 mm thick. There are 30 cylindrically shaped telescopes each covering 3.02 msr solid angle and 15 pyramid shaped telescope each covering 2.75 msr solid angle.

The light signal produced by energetic incident charged particle is transformed to an electronic signal by a 8 stage photo-multiplier tube. The fast/slow phoswich signal is shown schematically in Figure 2.8. The signal is separated into ΔE and E using a fast gate and a slow gate. The fast and slow signal are recorded separately using Lecroy FERA 4301b charge to digital converter. Two dimensional spectrum of ball fast signal (ΔE) vs. slow signal (E) in electronic channels is shown in Figure 2.4 and the forward array two dimensional spectrum is shown in Figure 2.5. The density of the scattering plots is proportional to the logarithm of the counts. The lines visible in the two dimensional spectra show the particle identification. The actual electronic resolution is 2048 by 2048 channels.

2.5 Data Reduction

The experimental data was stored event-by-event on 8mm magnetic tapes in the NSCL event buffer format. Because the MSU 4π Array is a permanent device with large number of detectors, the calibration and data reduction must be as standardized

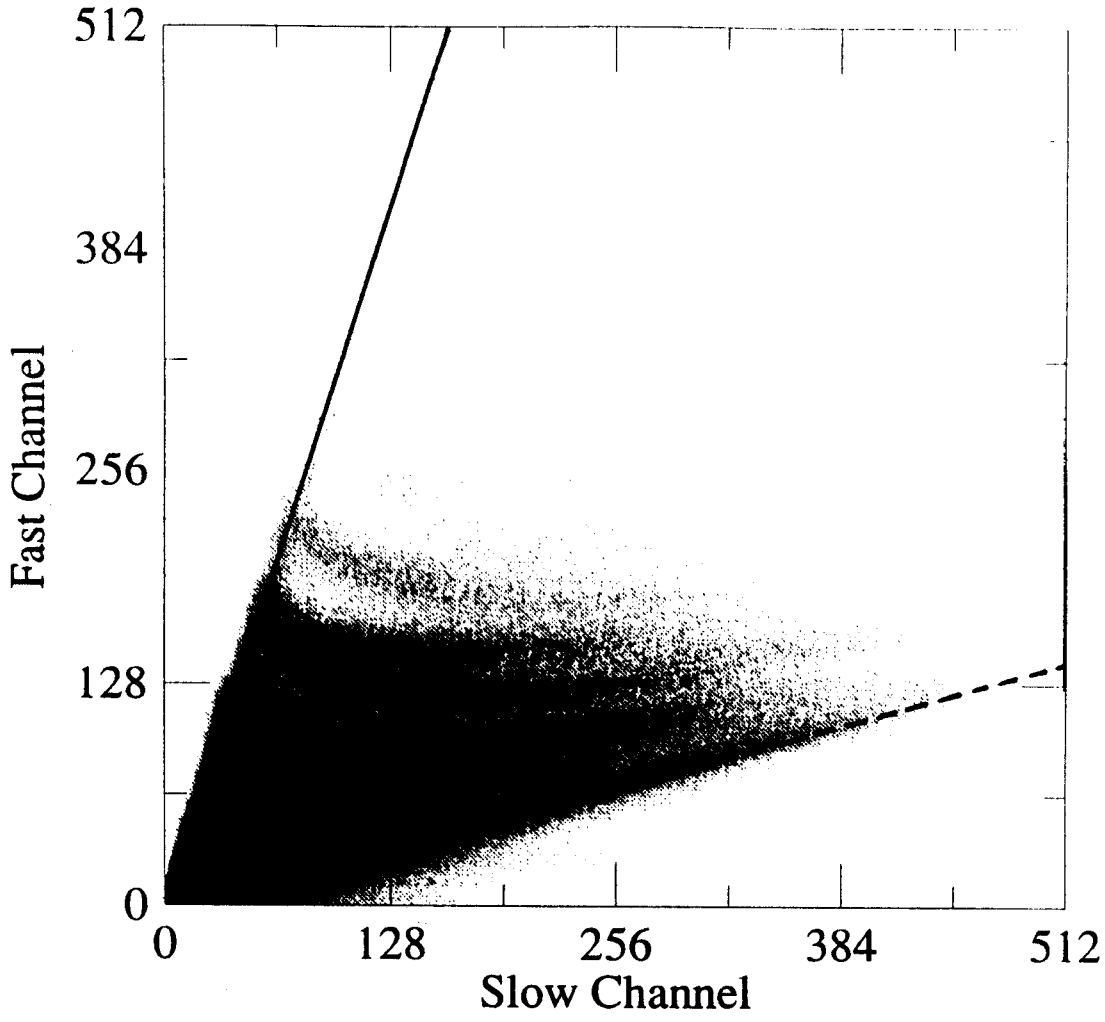

Figure 2.4: Ball phoswich fast electronic channel vs. slow electronic channel from Ar + Sc at 75 MeV/nucleon at 23°. The particles close to the solid line (punch-in line) are the particles stopped in fast plastic and the particles close to the dashed line (neutral line) are neutral particles.

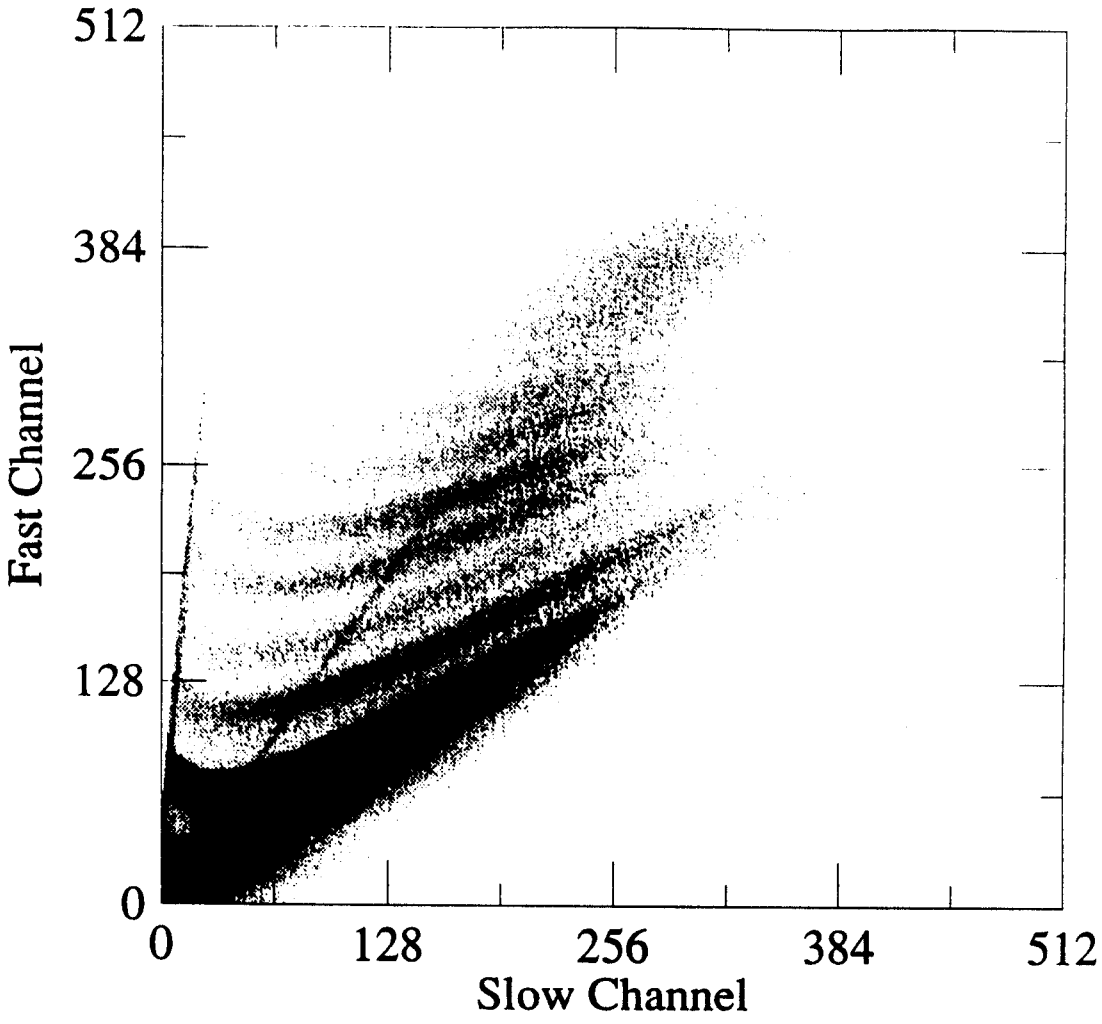

Figure 2.5: Fast electronic channel vs. slow electronic channel for a forward array detector at 7° for Ar + Sc at 75 MeV/nucleon.

as possible. To cope with the large number of detectors and the diverse experimental capabilities of the device, a calibrated template method is used for both the phoswich detectors and BCCs. The data reduction includes 3 steps:

- Using the energy response function obtained in calibration runs and the range-energy program (DONNA [Meye81]), we generate a standard line spectrum called a template (shown as Figure 2.9) and the corresponding look-up tables. For any point in the two dimensional template, the physical quantities such as Z, A, kinetic energy can be found from the tables.

- Matching all the two dimensional spectra of each detector to the template, we obtain a parameter file which contains all the information of the matching transformation from the original spectra to the matched spectra.

- Using the look up tables and the parameter files, we make physics tapes that contain information including multiplicity, particle charge number (Z), particle mass number (A), polar angle (θ), and azimuthal angle (ϕ) of all the events.

After the templates and look up tables are made, the energy calibration and particle identification is reduced to the relatively simple task of matching each detector to the template by varying the gain of the ΔE and E. A graphic matching program was used to use VAX workstation to obtain the gain parameters. The parameters of the matching is stored in a parameter file. The parameter file and look up tables are used to run the physics tape program for making physics tapes.

2.5.1 Phoswich Calibration

For a detector calibration there are two goals, to obtain the particle identification and to calibrate the kinetic energies for the identified particles.

The particle identification is done by using a standard spectrum and transforming the two dimensional spectrum of fast ΔE channel vs. slow E channels into a reduced two dimensional spectrum. A representative two dimensional histogram is shown in Figure 2.4. The particles close to the solid line, the punch-in line, are the particles stopped in the fast plastic. The non zero E channel on the punch-in line is due to the mixing of the fast and the slow light signal shown in Figure 2.8. The particles close to the dashed line are neutral particles. Thus the dashed line is called neutral line. The slope is also due to the mixing of fast and slow signals. The two dimensional histogram is transformed to the reduced channel, CH_f and CH_s using the following equation: [Cebr90a].

$$\begin{aligned} CH_f &= (\Delta E_{channel} - Y_0) - (E_{channel} - X_0)M_n \\ CH_s &= (E_{channel} - X_0) - (\Delta E_{channel} - Y_0)/M_p, \end{aligned} \tag{2.1}$$

where $\Delta E_{channel}$ and $E_{channel}$ are fast and slow electronic channels recorded from the experiment, the CH_f and CH_s are reduced channels which are proportional to the fast and slow light signal [Cebr90a], M_p and M_n are the slope of the punch-in line and the neutral line respectively, X_0 and Y_0 are the crossing point of the neutral line and the punch-in line, which represent the offset of the ADCs. Figure 2.6 shows a reduced two dimensional spectrum of CH_f vs. CH_s for a ball phoswich at angle 23° and Figure 2.7 shows a reduced two dimensional spectrum of forward array.

A set of gate lines are then calculated for the transformed two dimensional histogram to be used as a template for particle identification. The ball phoswich template is shown in Figure 2.9 and the forward array template is show in Figure 2.10. From the calibration runs, we get the following response function: [Cebr90a]

$$\begin{aligned} CH_s &= aE_s^{1.4}/A^{0.4}Z^{0.8} \\ CH_f &= bE_f^{0.5} - c, \end{aligned} \tag{2.2}$$

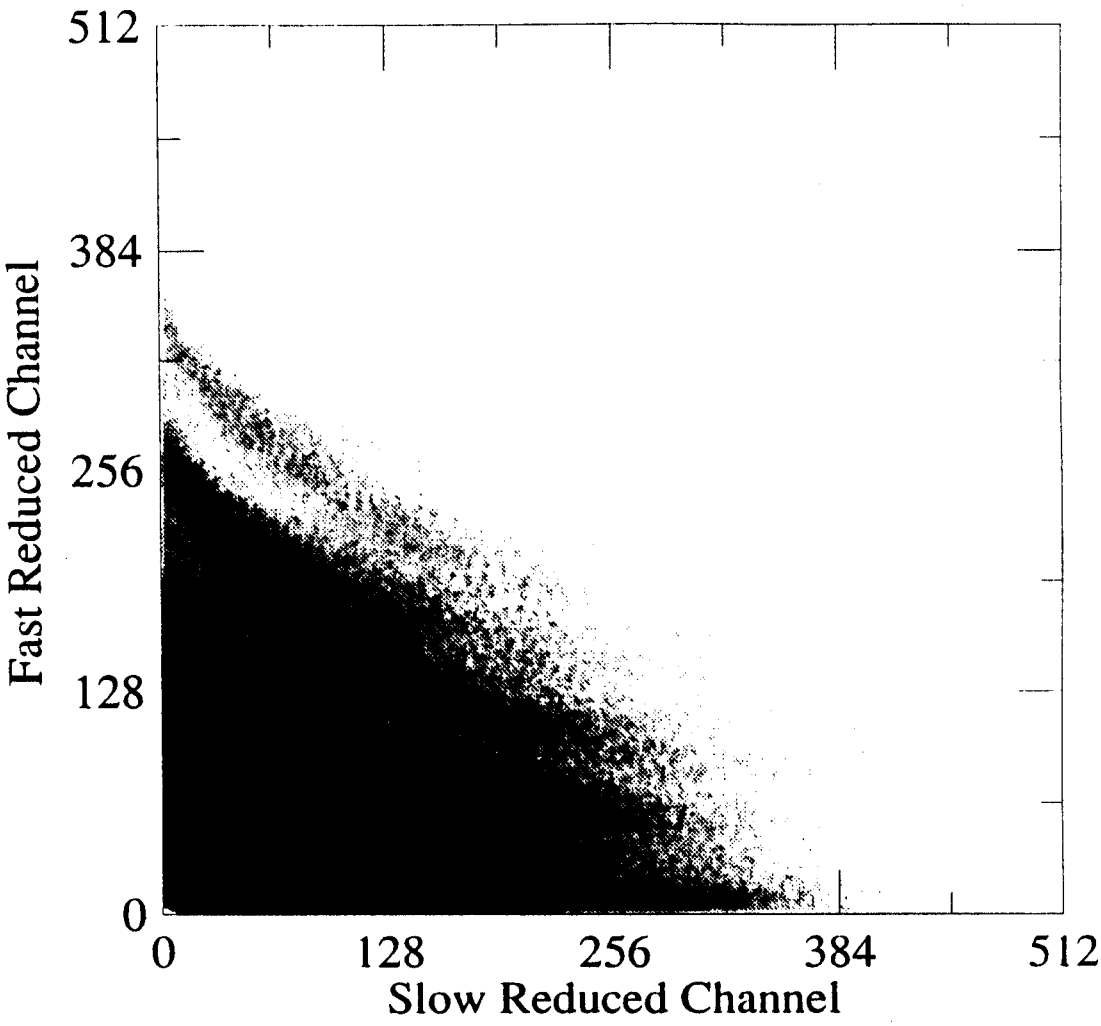

Figure 2.6: Fast reduced channel vs. slow reduced channel for a ball phoswich detector at 23° for Ar + Sc at 75 MeV/nucleon.

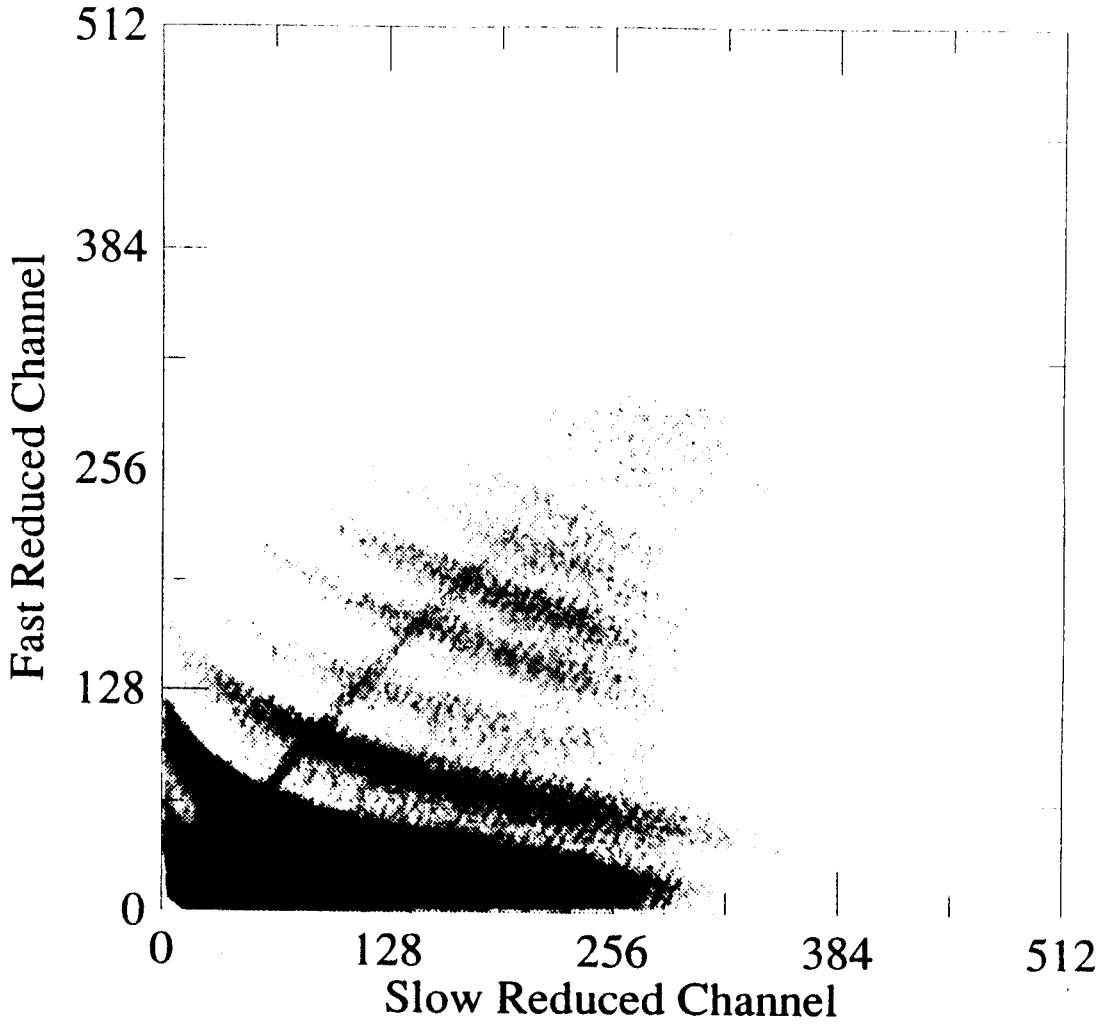

Figure 2.7: Fast reduced channel vs. slow reduced channel for a forward array detector at 7° for Ar + Sc at 75 MeV/nucleon.

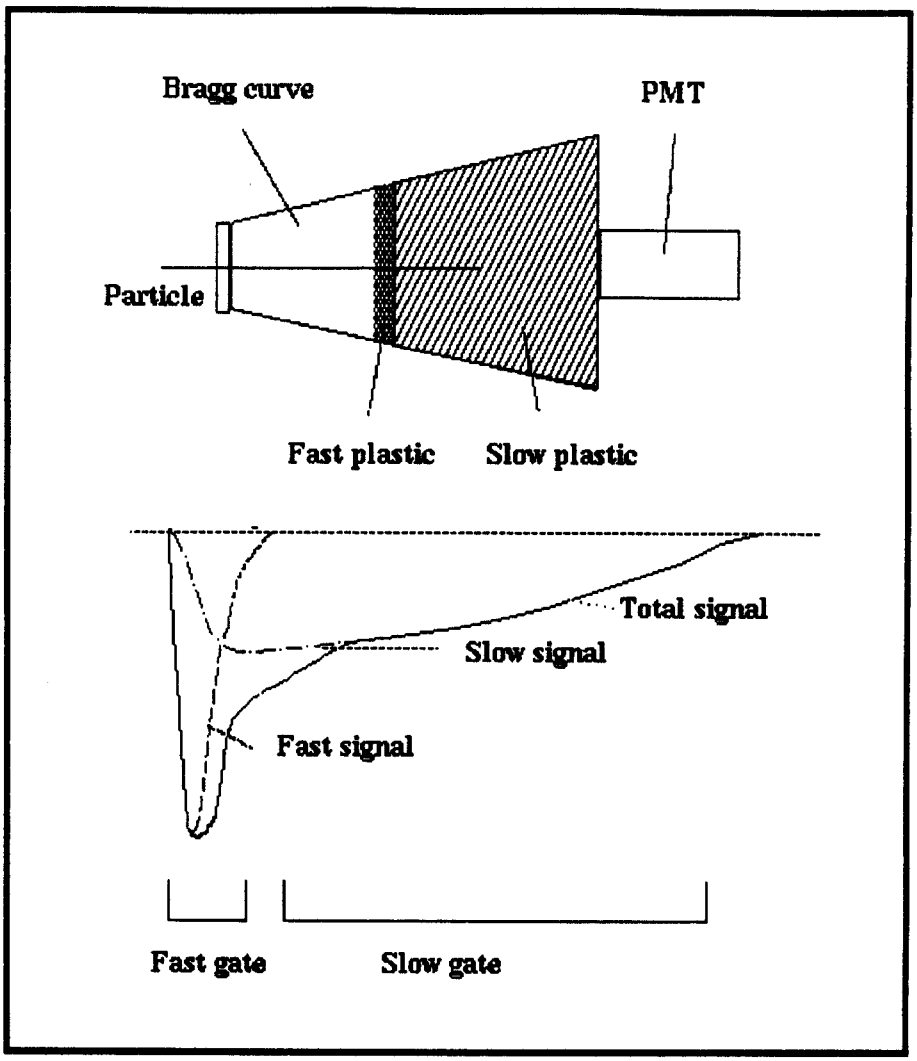

Figure 2.8: The fast/slow plastic telescope, the signals and the gates.

where the CH_s and CH_f are the slow plastic and fast plastic reduced channels, E_s and E_f are the particle energy loss inside the slow and fast plastic, respectively. The quantities a, b and c are the gains and offsets which are determined by fitting the measured spectra to the response function through range-energy calculations. The range-energy program called DONNA [Meye81] was used. For a given particle of Z and A with certain kinetic energy, the E_s and E_f are calculated using DONNA given the density and the thickness of all the material along the particle path. Therefore for a given particle with Z and A one can calculate the relation of CH_s vs. CH_f shown as Figure 2.11. From bottom to top, the curves are for proton, deuteron, triton and Z=2 to Z=8 (with the most probable isotope A). We fit the calculated particle lines of 2.11 on the particle lines of the experimental two dimensional spectrum 2.4, we obtain the constant a, b and c.

From the template gate lines we can identify the Z and A of a particle. To reduce computational time for physics tape program, a look-up table with 512 by 512 resolution was made which gives particle Z (charge number) and A (mass number) according to the slow and fast electronic channels. The most probable isotope mass number for $Z > 1$ was used. Along with the particle identification table, a template is also made in 512 by 512 resolution to be used as a standard spectra for matching the experimental data. The ball template is shown in Figure 2.9 and the forward array template shown in Figure 2.10. The solid lines are the gate lines.

Two sets of tables and templates are made for ball phoswich detectors and forward array phoswich detectors separately. Then the experimental two dimensional spectra of 215 detectors for each beam energy are matched into the template using the matching program. The gain factors and offsets are then written in the parameter files.

Combining the response functions (equation 2.2), using the constants obtained by

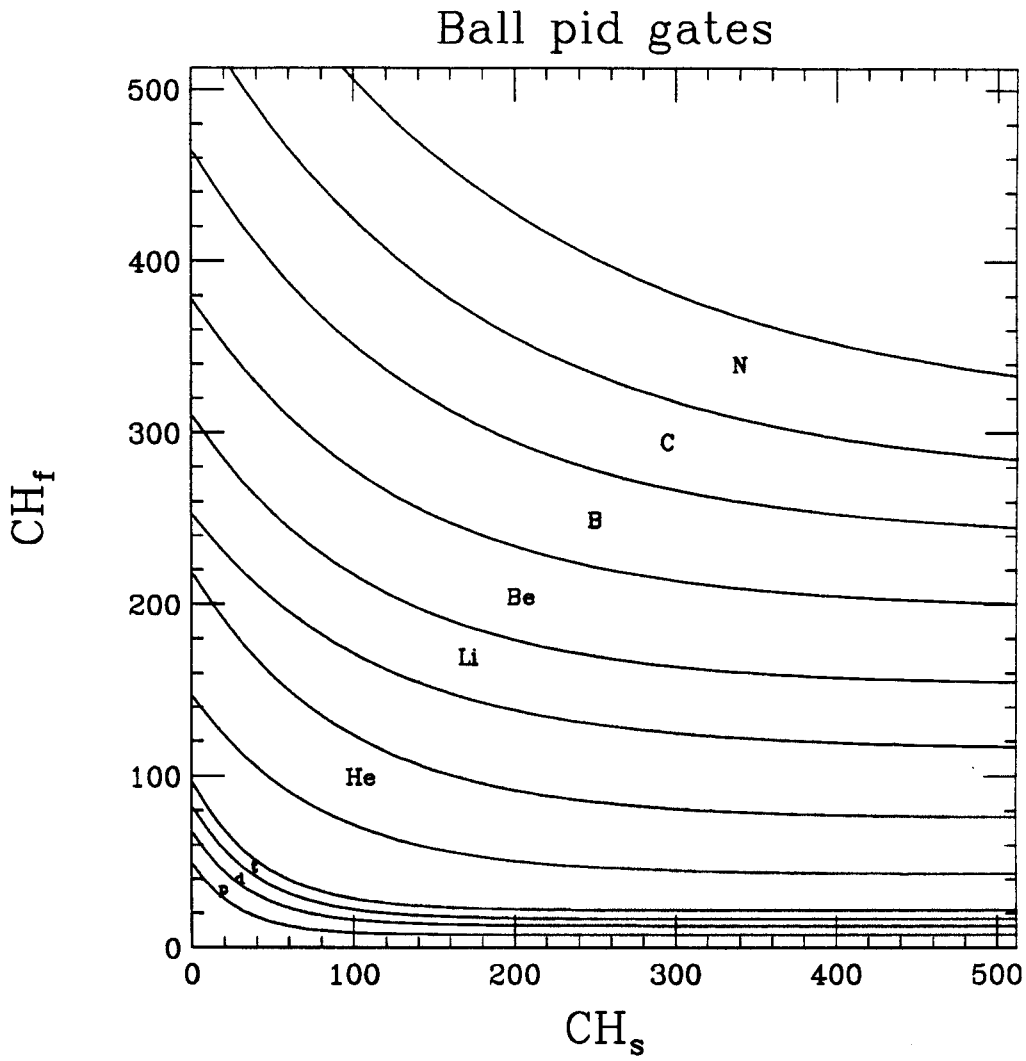

Figure 2.9: The particle gate lines for p,d,t and Z=3 to 4 with the most probable isotopes.

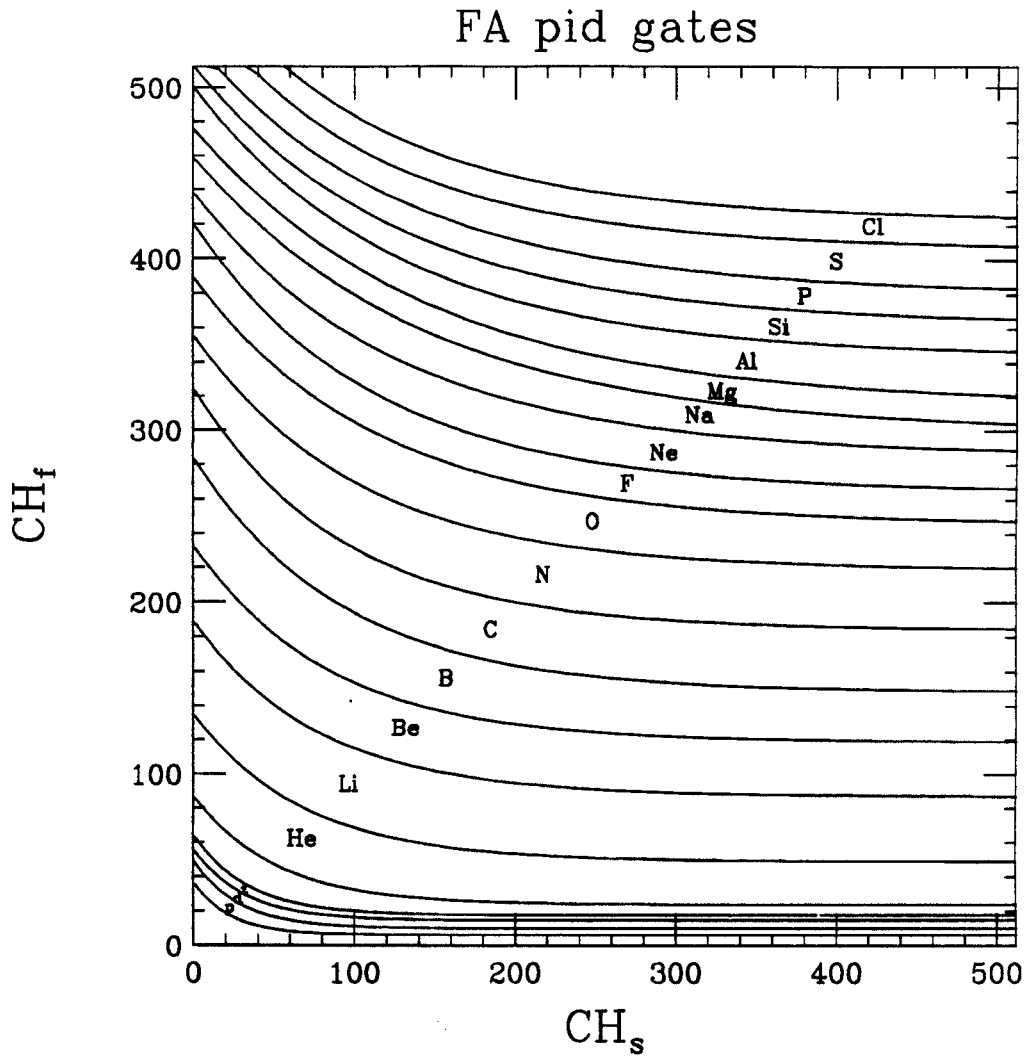

Figure 2.10: The particle gate lines for p,d,t and Z=3 to 4 with the most probable isotopes for forward array detectors.

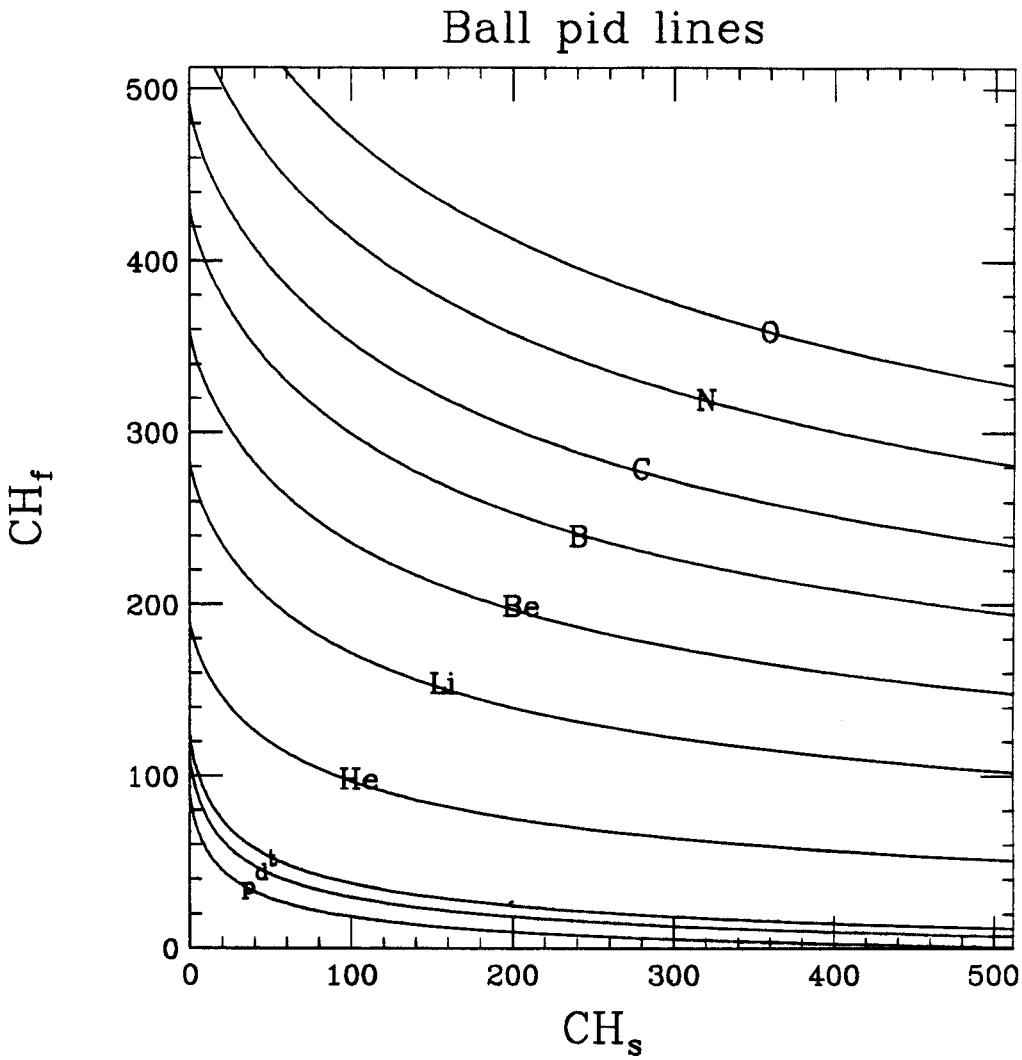

Figure 2.11: The particle lines for p,d,t and Z=3 to 4 with the most probable isotopes calculated from energy loss and response function.

the fitting, and the range-energy program (DONNA), one can determine the incident energy of the particle. Then an energy table was made to convert the channel numbers to incident particle kinetic energy.

2.5.2 Bragg Curve Calibration

Prior to the mass production of all 32 BCCs (30 working modules and two spares), a prototype module was made and a calibration run was performed [Cebr91]. The calibration run was done at NSCL using a beam of ^{40}Ar produced by the K500 cyclotron. The prototype module was placed inside the S320 spectrometer. A 4 MeV/nucleon ^{40}Ar was stopped in the gas counter and an energy resolution of 2% was determined by the ratio of FWHM(full with half maximum) and the beam energy. Then a 35 MeV/n ^{40}Ar beam bombarded an target 15 cm away from the entrance window of the BCC. For the particle stopped inside the gas counter, the charge number can be identified by BCC's E signal vs. Z signal as shown in Figure 2.12. For the particle punching through the gas counter and stopping inside the fast plastic of the phoswich, the charge number (Z) of the particle can be identified by the BCC's E channel vs. ΔE (fast plastic) channel as shown in Figure 2.13. Clear Z lines from proton to Mg can be seen. To study the energy response function, the fragments produced by the reaction of Ar + Au were selected by the spectrometer at different rigidities. The result of the study shows that the energy response of the detector is linear and independent of the charge and mass of the incident particle (Figure 2.14) [Cebr91])

The same method was used to calibrate the two dimensional spectra of BCCs' E signal vs. fast plastic signal channel as for the fast/slow plastic. The response function of a particle stopped in the fast plastic is the same as the response function of a particle stopped in slow plastic and the response function of BCC is linear as